REPORT NO. DOT - TSC - FAA - 71 - 5



# THE IMPACT OF INERTIAL NAVIGATION ON AIR SAFETY

R.M. HERSHKOWITZ
D. O'MATHUNA
K.R. BRITTING

TRANSPORTATION SYSTEMS CENTER
55 BROADWAY
CAMBRIDGE, MA. 02142

MAY 1971
TECHNICAL REPORT



Prepared for

FEDERAL AVIATION ADMINISTRATION
WASHINGTON, D.C. 20590

| 1. Report No. | 2. Government Accession No. | 3. Recipient's Catalog No. |
|---|---|---|
| 4. Title and Subtitle<br>The Impact of Inertial Navigation on Air Safety | | 5. Report Date<br>May 1971<br>6. Performing Organization Code |
| 7. Author(s) R.M. Hershkowitz, D. O'Mathuna and K.R. Britting | | 8. Performing Organization Report No.<br>DOT-TSC-FAA-71-5 |
| 9. Performing Organization Name and Address<br>U.S. Department of Transportation<br>Transportation Systems Center<br>Cambridge, Massachusetts 02142 | | 10. Work Unit No.<br>R1032<br>11. Contract or Grant No.<br>FA04<br>13. Type of Report and Period Covered |
| 12. Sponsoring Agency Name and Address<br>Federal Aviation Administration<br>Washington, D.C. 20590 | | Technical Report<br>14. Sponsoring Agency Code |
| 15. Supplementary Notes<br>Presented to Institute of Navigation on April 14, 1971 | | |

16. Abstract An analysis of inertial navigation system performance data was carried out to assess the probable impact of inertial navigation on the aircraft collision risk in the North Atlantic region. These data were used to calculate the collision risk between two aircraft flying at the same nominal flight level on adjacent tracks. The inertial system's error sources are treated in a statistical sense to infer the en route error behavior from the terminal error data. Collision risk estimates are derived for easterly and westerly transatlantic flights. The results of this relatively conservative analysis show that there is strong evidence to support the concept that the widespread use of inertial navigators will lead to reduced separation standards in the North Atlantic region while maintaining present safety standards.

| 17. Key Words | 18. Distribution Statement |
|---|---|
| •Inertial navigation<br>•Collision risk model<br>•En route navigation statistics<br>•Blunders | Unclassified — Unlimited |

| 19. Security Classif. (of this report) | 20. Security Classif. (of this page) | 21. No. of Pages | 22. Price |
|---|---|---|---|
| Unclassified | Unclassified | 25 | |

# THE IMPACT OF INERTIAL NAVIGATION ON AIR SAFETY

by

R.M. Hershkowitz, D. O'Mathuna
U.S. Department of Transportation, T.S.C.
Cambridge, Mass.

and

K.R. Britting
M.I.T. Measurement Systems Laboratory
Cambridge, Mass.

## INTRODUCTION

In the coming years, the expected increase in traffic density in the North Atlantic (NAT) region will create pressure for a reduction of the separation standards currently in operation. Any such reduction must not cause an undue increase in risk of collision. This report analyzes inertial navigation performance and assesses its ability to reduce collision risk in the NAT region.

Though the routing system involves separation in three dimensions - and, in the case of a composite system, the diagonal separation requires special treatment - we shall, in the present investigation, confine our analysis to the lateral separation.

In the next section, an INS input error model is presented along with a description of a terminal data study conducted by Air France. The model and the data are then combined in order to infer the en route inertial error characteristics. The collision risk model, adopted by the North Atlantic Systems Planning Group (NATSPG)[6-10], is then discussed. An adjusted formula for the expected number of accidents is combined with the en route errors to yield an estimate on the risk associated with specific separation standards. The final section includes a summary and discussion of the results.

## EN ROUTE INS ANALYSIS

### Data Base

The data were collected by Air France over its North Atlantic routes between July, 1968 and April, 1970 with 29 inertial navigation systems.[1] A total of about 24,000 hours of navigation time was logged during 1528 flights. The inertial navigation system was the Litton LTN-51, a free (wander)-azimuth two-dimensional navigator, two of which were installed in each aircraft. Since no en route navigational fixes were available, the navigational accuracy was determined at only the terminal point.

Figures 1 and 2 show the distribution of radial errors for the easterly and westerly flights, respectively. Two distributions for the operational navigation errors are shown for each flight path: an average distribution, $R_A$, and a maximum distribution, $R_M$.

In cases where an inflight failure or a large deviation (radial error greater than 50n.m. at arrival) of only one of the two inertial systems occurs, the operational radial error is taken to be the radial error associated with the in-spec. system, i.e. $R_A=R_M$. This neglecting of the out-of-spec. errors in the statistical evaluation is justified on the basis that the flight crews were, in all cases, able to detect that the system had failed or was exhibiting large errors.

In situations where both of the systems have greater than a 50 n.m. radial error at arrival, $R_M$ and $R_A$ are calculated from the following:

$$R_M = R_A = \tfrac{1}{2}\left[\left(X_1+X_2\right)^2+\left(Y_1+Y_2\right)^2\right]^{1/2} \qquad (1)$$

where

$X_k$ = lateral error associated with system k, k = 1, 2

$Y_k$ = longitudinal error associated with system k, k = 1, 2.

Finally, for the case of nominal operation, the radial errors were calculated using:

$$R_M = \text{maximum}\left(R_1, R_2\right) \tag{2}$$

$$R_A = \tfrac{1}{2}\left[\left(X_1+X_2\right)^2 + \left(Y_1 + Y_2\right)^2\right]^{1/2} \tag{3}$$

For each point on the distribution curves, the ordinate, when divided by 100, can be interpreted as the probability that the radial error for a given flight will not exceed the abscissa value. Table 1 presents values for the radial error in nautical miles for several important points.

| Prob. radial error is less than.. | Easterly | | Westerly | |
|---|---|---|---|---|
| | $R_A$ (n.m.) | $R_M$ (n.m.) | $R_A$ (n.m.) | $R_M$ (n.m.) |
| .683 | 5.8 | 10.6 | 6.2 | 12.0 |
| .757 | 6.6 | 12.0 | 7.7 | 14.8 |
| .941 | 11.7 | 20.0 | 12.4 | 20.4 |
| .950 | 11.9 | 20.8 | 12.7 | 21.0 |
| .990 | 23.0 | 36.0 | 20.0 | 30.0 |

TABLE I
EASTERLY-WESTERLY RADIAL ERROR COMPARISON

The decay of the terminal distribution curves lies between exponential and Gaussian. If the empirical distribution were assumed to be Gaussian, the 68.3% and 95% points would correspond to the one and two standard deviation points, respectively. If the exponential assumption were used, the 75.7% and 94.1% points would correspond to the one and two standard deviation points, respectively.

Comparison of Figs. 1 and 2 reveals that although the average time of flight for the westerly route is 1.17 hours longer than the time of flight for the easterly route, the westerly radial errors are only slightly larger than the easterly radial errors. For example, at the Gaussian one standard deviation ($1\sigma$) point the average easterly radial error is 5.8/7.33 = 0.79 n.m./hr. while the corresponding

westerly error is only 6.2/8.5 = .73 n.m./hr. In all probability, the observed better performance for westerly flights is achieved because the systems' inertially referenced angular velocity is smaller than for easterly flight. This results in a low system sensitivity to gyro torquer uncertainty.

## Inference of En Route Errors from the Terminal Errors

### Approach to the Problem

As has been previously discussed, the data base consists exclusively of terminal error statistics. In order to calculate the collision risk between two aircraft occupying the same flight level and flying on adjacent tracks, it is necessary to know the error distributions for the entire time of flight. It is, therefore, necessary to infer the en route errors from the terminal errors.

If accurate statistical estimates of the major inertial system uncertainties are available, then the en route behavior can be obtained from the terminal data through the use of straightforward simulation techniques. That is, the inertial system's time-varying statistical behavior is determined through statistical error analysis techniques[2], matching the simulation results to the empirical data. This type of analysis is complicated by the fact that the error statistics of inertial systems are non-stationary. This characteristic is due to the fact that inertial systems have undamped oscillatory characteristics which prevent the attainment of steady state conditions and also the fact that the linearized inertial system equations are time-varying. The analysis techniques associated with optimal control theory would appear to be ideally suited to a problem of this nature. Such techniques are being developed for this application, but have not reached fruition.

For the purposes of this paper, however, a simplified, albeit conservative, approach is taken such that the en route statistics can be expeditiously obtained and the collision risk formulae utilized to yield a tentative conclusion as to the affect of inertial system technology on air safety. Specifically, the inertial navigation system is simulated for the situation where the error uncertainties are modelled as being members of an ensemble of constant functions.[4] Furthermore, the error equations are solved for the case of constant east-west velocity at constant latitude, a reasonable assumption given the North Atlantic traffic structure. As is shown in Appendix A, the constant velocity assumption results in the inertial system's error differential equation having constant coefficients.

## Inertial System Simulation

The Litton LTN-51 system was simulated using the error model shown in Appendix A for the case of constant east-west velocity of 637 knots at a constant latitude of 45°. As indicated, the major error sources consist of the gyro drift uncertainties, (u)$\underline{\omega}$, the accelerometer uncertainties, (u)$\underline{f}$, the gyro torquer scale factor uncertainties, $\tau_x$ and $\tau_y$, and the initial platform misalignments, $\varepsilon_N(0)$, $\varepsilon_E(0)$ and $\varepsilon_D(0)$. The system response to each of these error uncertainties, which were modelled as being members of an ensemble of constant functions, was separately determined. Assuming zero correlation among the error sources, the resulting latitude errors (the cross track error for this case) were squared, summed, and the square root was taken. The resulting root-sum-squared plots are shown in Figure 3 for the following error source magnitudes:

Gyro drift: $(u)\omega_k$ = 1 meru (0.015 deg/hr.), k = x,y,z

Accelerometer: $(u)f_k = 10^{-4}g$, k = x,y

Gyro torquing: $\tau_k = 10^{-3}$, k = x,y

Platform misalignment: $\varepsilon_k(0)$ = 1 arc-min; k = N,E,D.

In the above, the x,y,z subscripts refer to uncertainty components occurring along the platform's x,y, and z axes. Note that since two-degree-of-freedom gyroscopes are used, the three dimensional gyro drift vector is associated with only two instruments.

For the westerly flight, the dominant error for the first several hours is caused by the initial platform misalignments while the long term error is dominated by effects due to gyro drift. For the easterly flight, on the other hand, the long term error is dominated by a combination of gyro drift and torquing uncertainty. Obviously, the shape of the latitude error curves depends on the assumptions made as to the relative weighting of the error sources.

The theoretically derived en route error curves were then scaled to match the empirically determined terminal data - and our assumption as to its distribution shape. This was a two step process. First, the radial errors were scaled in accordance with the ratio of the terminal errors to the theoretical errors at the terminal point. Then, since the data consisted exclusively of radial error statistics, the radial error had to be apportioned into equivalent latitude and longitude errors. This apportionment was performed on the basis of the error simulation which showed that the latitude and longitude errors were approximately equal at the terminal points.

The scaling factors resulting from the above considerations are given in Table 2 below.

| Assumption on Tail Shape of Distribution | Type of Radial Error | DIRECTION OF FLIGHT Easterly | Westerly |
|---|---|---|---|
| Gaussian | $R_A$ | .57 | .56 |
| Gaussian | $R_M$ | 1.04 | 1.08 |
| Exponential | $R_A$ | .65 | .70 |
| Exponential | $R_M$ | 1.18 | 1.35 |

TABLE II
SCALING FACTORS FOR EN ROUTE ERRORS

The same scaling methods were used to determine the cross track velocity error associated with the position error.

Figure 4 represents the theoretical average velocity information assuming a Gaussian terminal distribution. Similar plots can be derived for the three other cases by rescaling the theoretically derived en route error curves (i.e., multiplying the given "average - Gaussian" curves by the ratio of the scale factor for the desired case to the scale factor for the "average - Gaussian" case).

It is to be emphasized that the en route determination used herein tends to be conservative since modelling the gyro drift as a member of the ensemble of constant functions results in an approximately linear error growth. Other, more accurate, gyro drift models which involve random walk processes[5], result in navigation errors which grow proportional to the square root of time.

## COLLISION RISK CALCULATIONS

### Collision Risk Equation

The effects of the en route Inertial Navigation statistics derived above are assessed by considering the collision risk associated with specific lateral separation standards. A model has been developed by P. G. Reich[6-8] and adopted by the North Atlantic Systems Planning Group (NATSPG)[9-10], which relates the expected number of accidents in 10 million hours of flying to aircraft characteristics, separation standards, and flying errors.

An adaptation of this model has been used to analyze the number of accidents expected to occur in an airspace containing inertially-equipped air carriers only. This adaptation consists of the admission of time and direction dependences to the original formulation. For the number of accidents due to a loss of lateral separation, the adjusted

formula, which is discussed in more detail in Appendix B, is given by:

$$N^*_{ay} = 10^7 \Bigg\{ E_y(\text{opp}) P_y(\text{opp}) \left[ \frac{1}{S_x} \left( \bar{V} P_z(0) + \lambda_x N_z(0) + \frac{\lambda_x \overline{|\dot{y}(\text{opp})|}}{2\lambda_y} P_z(0) \right) \right]$$

$$+ E^e_y(\text{same}) P^e_y(\text{same}) \left[ \frac{1}{S_x} \left( \frac{1}{2}\overline{\Delta V} P_z(0) + \lambda_x N_z(0) + \frac{\lambda_x \overline{|\dot{y}^e(\text{same})|}}{2\lambda_y} P_z(0) \right) \right]$$

$$+ E^w_y(\text{same}) P^w_y(\text{same}) \left[ \frac{1}{S_x} \left( \frac{1}{2}\overline{\Delta V} P_z(0) + \lambda_x N_z(0) + \frac{\lambda_x \overline{|\dot{y}^w(\text{same})|}}{2\lambda_y} P_z(0) \right) \right] \Bigg\}^* \quad (4)$$

where the asterisk denotes the average over the time of flight for the quantities concerned. In the above, the superscripts e and w denote east and west directed flights respectively, and

$E_y$ (same/opp) = the percentage of time in which two aircraft are proximate.

$P_y$ (same/opp) = the probability that two aircraft, nominally separated by the lateral separation standard, $S_y$, overlap in the lateral dimension.

$\dot{y}$ (same/opp) = the average relative lateral velocity of two aircraft during lateral overlap.

$S_x$ = the along-track separation standard

$P_z(0)$ = the probability that two aircraft, nominally at the same altitude, will overlap in the vertical dimension.

$N_z(0)$ = the relative frequency with which two aircraft nominally at the same altitude, will overlap in the vertical dimension.

$\bar{V}$ = the average speed of the aircraft under consideration.

$\overline{\Delta V}$ = the average difference in along-track speed between two aircraft in adjacent lanes.

$\lambda_y$ = the lateral dimension of the aircraft.

$\lambda_x$ = the longitudinal dimension of the aircraft (which can be extended to include vortex overlap distance).

Remarks on the Treatment of Large Flying Errors

"It is the large rare errors (rather than those of moderate size which forms the bulk of observations) that mainly determines the risk of collision."[6] The fact that the treatment of these errors are critical to the analysis of expected accident levels explains the emphasis placed in the literature[7][9] upon the careful modelling of the tails of the error distribution. Of particular importance, in this regard, is the inclusion of all significant sources of such error.

There are two general sources of large error to be considered in investigating the flying density of inertially-equipped carriers. The first type, which we will refer to as "blunders" might arise either from a system breakdown such as a specific mechanical or electrical failure or from an incorrect set of input instructions such as faulty way-point or initial position information. The second type, occurring in the absence of two first type errors, is assumed to be a statistical characteristic of the system itself; namely, there is a finite, albeit small, probability that an operating system will, upon occasion, exhibit large errors.

The exclusion of certain blunder errors in the data reduction (as in the case of an inflight failure or large deviation of only one of the two on-board inertial systems) and the lack of sufficient data preclude a thorough analysis of blunder errors at this time. Therefore, for our investigation, we shall assume that the navigation errors arise solely from the characteristics of the navigation system itself, even though it appears certain that blunder errors are inherently included in the data. From the viewpoint of assessing the navigation system accuracy itself, this is a conservative assumption. However, for the broader question of estimating risk, this assumption is likely to lead to optimistic conclusions. This matter is discussed further in the "Summary and Discussion of Results" section.

Presentation of Results

$N^*_{ay}$ is calculated for each of the four cases discussed in section 2 (i.e., average-Gaussian, average-exponential, maximum-Gaussian, and maximum-exponential). The details are presented in Appendix B. The relationship between the risk, as reflected in the value for $N^*_{ay}$, and the lateral separation standard, $S_y$ are graphically presented in figures 5 and 6. These values are compared with the target levels of

safety specified by NATSPG for "the assessment of future separation standards over the North Atlantic."(9)

## SUMMARY AND DISCUSSION OF RESULTS

### Current Results

The results of the analysis of the risk due to Inertial Navigation Errors are presented in Figures 5 and 6. We see that in the most optimistic case, namely where the average error is associated with a Gaussian distribution, the target level of safety can be achieved with a separation of approximately 15 n.m. On the other hand, for the most pessimistic case, where the maximum error is associated with an exponential distribution, the safety target requires approximately a 45 n.m. separation. The intermediate assumptions of maximum with Gaussian and average with exponential are seen to yield required separations of 37 n.m. and 25 n.m. respectively.

In view of the conservative nature of the navigation model and the presence of some blunder statistics in the data, it appears plausible that the inertial navigation system, in the absence of blunders, is accurate enough to meet safety requirements with a separation standard of 30 n.m. or less. It appears reasonable that, even with the inclusion of blunders into our analysis, INS technology will allow for a substantial reduction of the present 90 n.m. set for safety.

This possible reduction in separation standards afforded by the introduction of inertial systems has been anticipated. The present analysis provides some quantitative corroboration. A more precise and reliable estimate of this reduction will require the further studies discussed below.

### Future Efforts

There are three aspects of the problem requiring further investigation before any definite statements can be made concerning the full impact of inertial navigation systems on safety in the North Atlantic. Initially, a study is in order to determine the magnitude and likelihood of blunder errors and estimate their significance, particularly in relation to system equipment reliability checkout procedures and operational procedures. Secondly, a careful study of externally-aided inertial systems is called for. Such systems appear to promise greater reliability (in terms of independent position checks) and greater accuracy (in terms of en route updating of inertially-derived position.) Finally, a more detailed analysis of the en route navigation statistics will eventually be required.

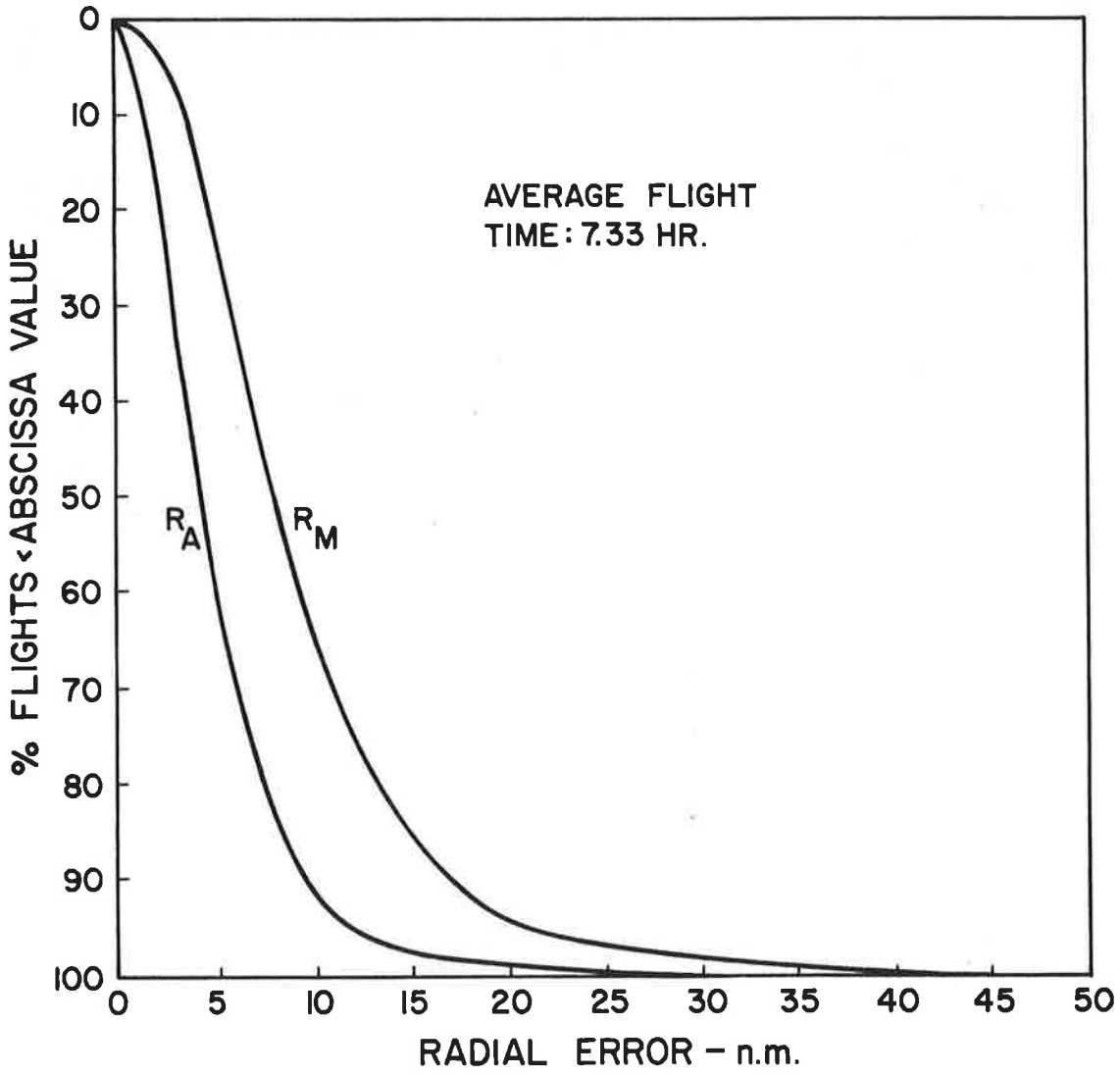


Figure 1. Radial Error Distribution - Easterly Flights

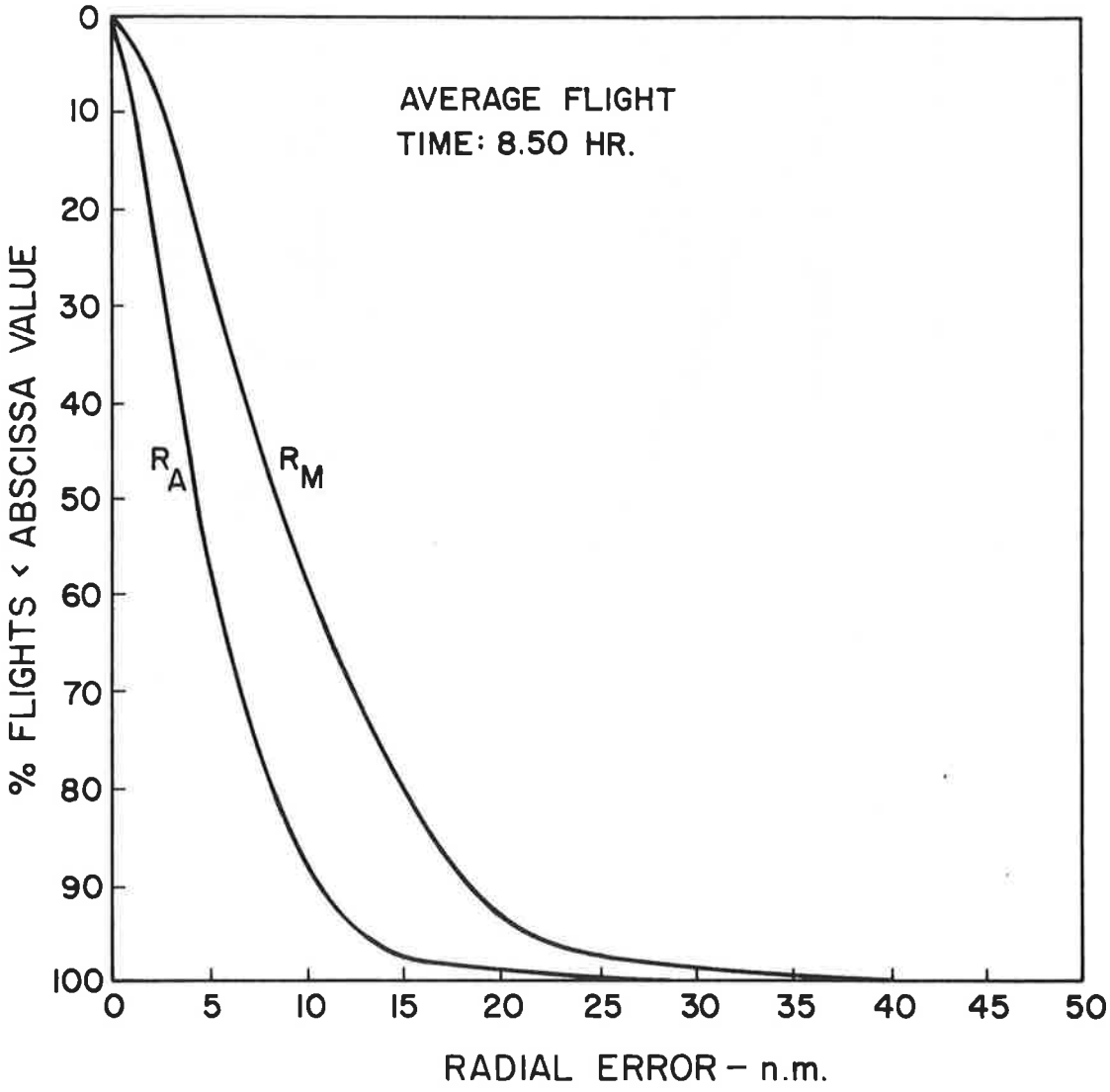


Figure 2. Radial Error Distribution - Westerly Flights

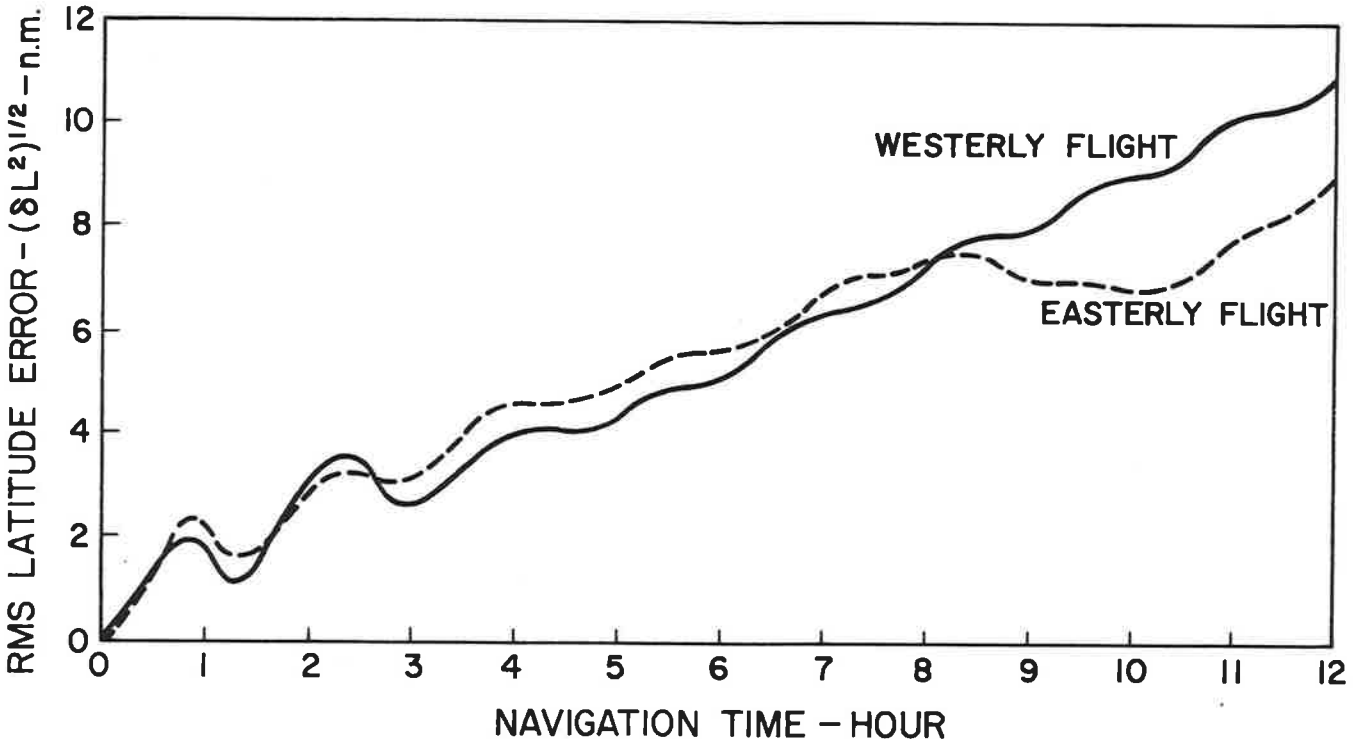


Figure 3. RMS Position Latitude Error for Free Azimuth Inertial Navigation System
(Gaussian - Average Case)

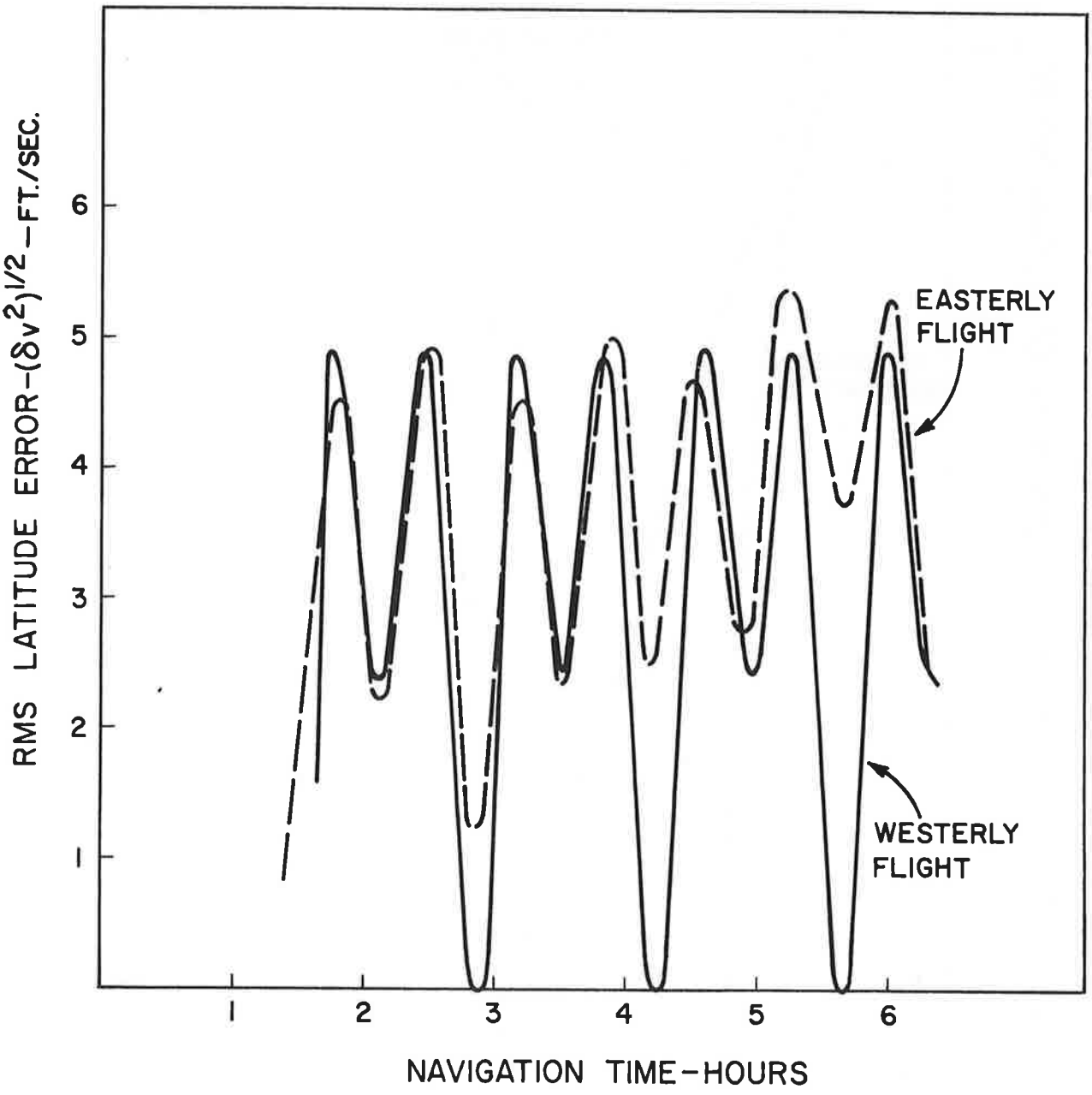


Figure 4. RMS Velocity Latitude Error for Free Azimuth Inertial Navigation System (Gaussian - Average Case)

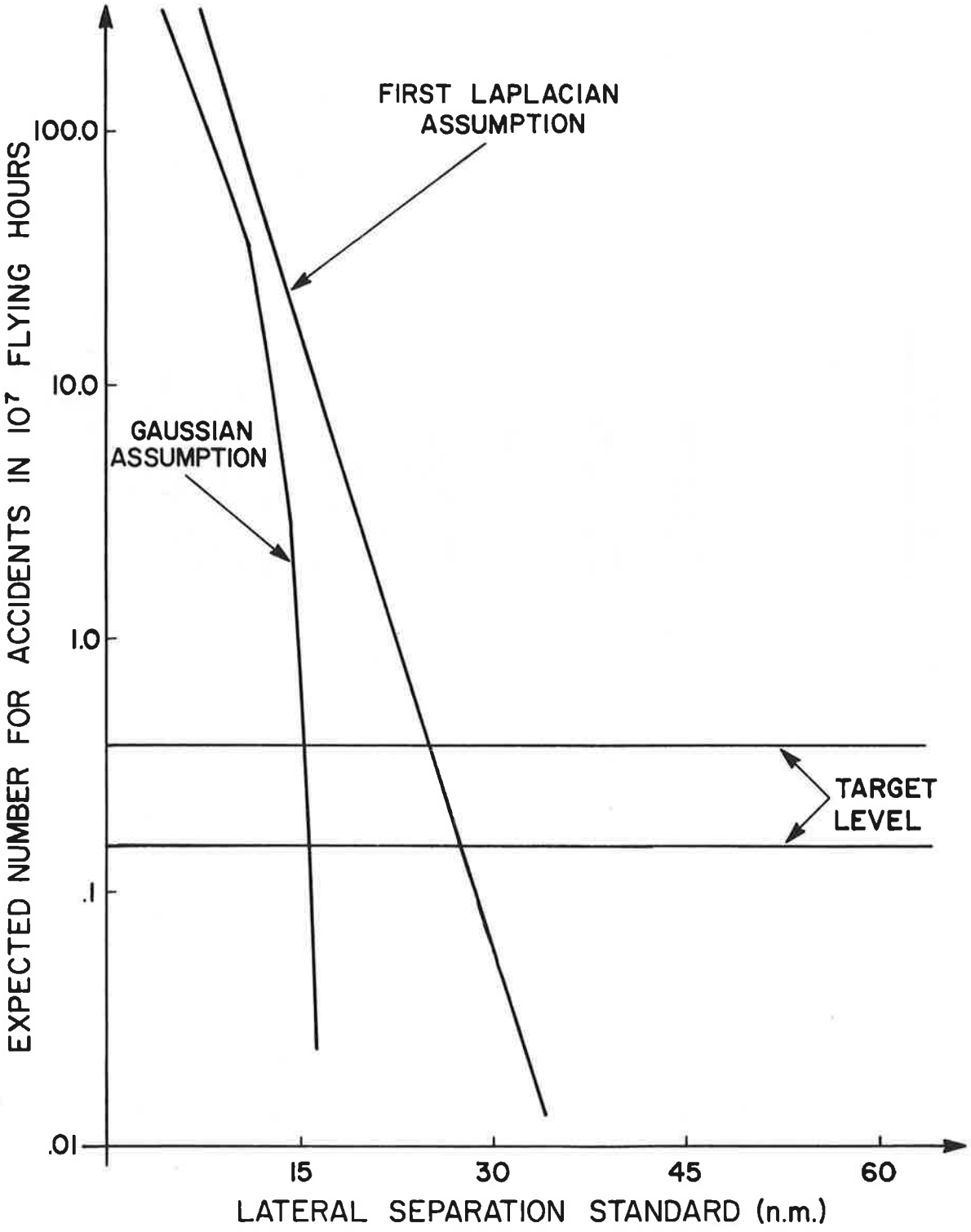


Figure 5. Accident Level vs. Lanewidth
(Using Average Distributions)

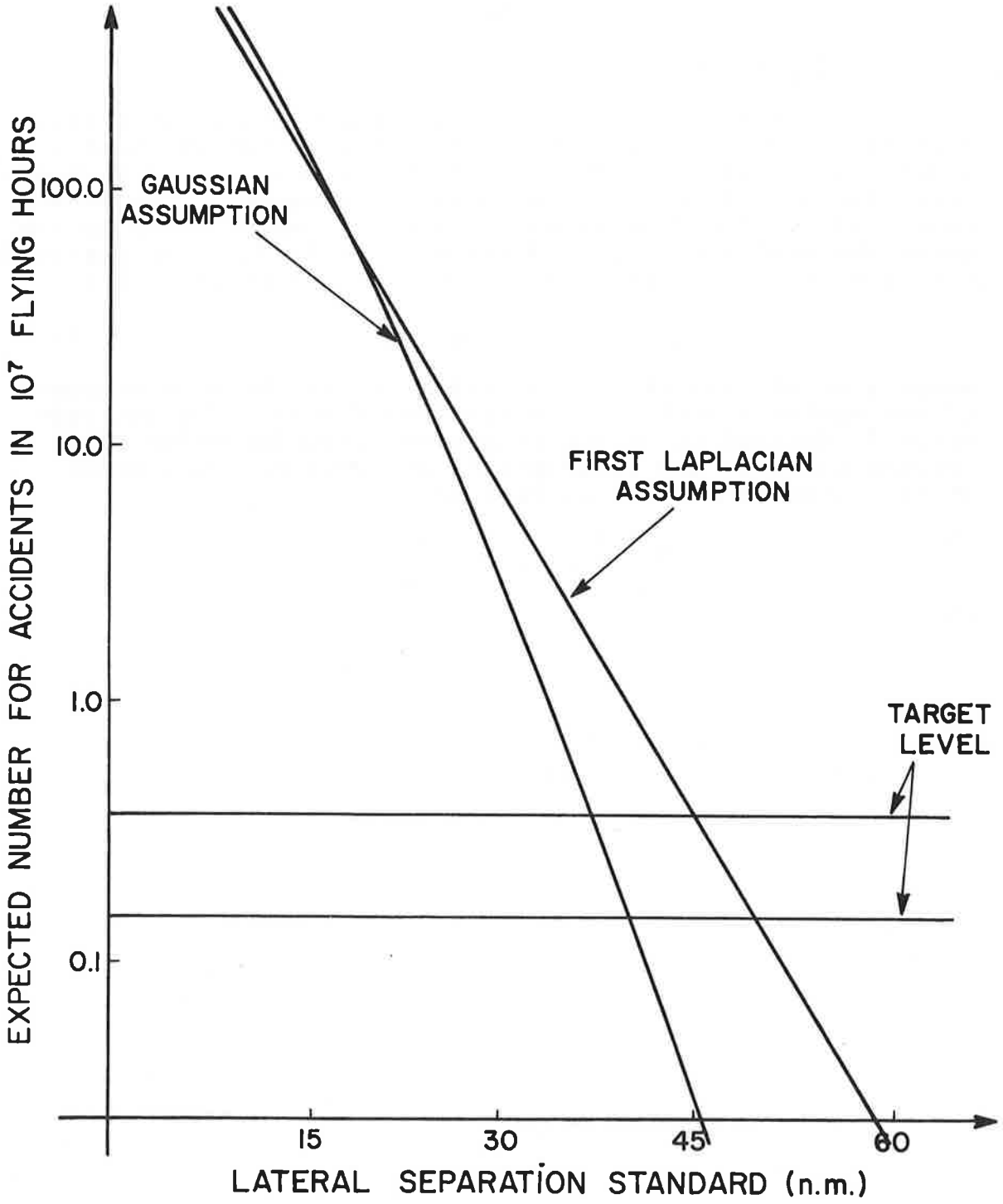


Figure 6. Accident Level vs. Lanewidth
(Using Maximum Distributions)

## APPENDIX A

### INERTIAL SYSTEM MODEL

The Litton LTN-51 inertial navigation system is a free azimuth two-dimensional navigator. This system utilizes a local level platform with a space stabilized azimuth channel, (3) i.e., the azimuth or vertical gyro is untorqued. The error equations for the free azimuth system are obtained by specializing the rather generalized theory in Ref. (4). In particular, the error equation for this class of system is given by:

$$\underline{\Lambda}\ \underline{x} = \underline{Q} \tag{A-1}$$

where $\underline{x}$ is the system's error state vector which is composed of the system's attitude and position errors. The attitude error is defined to be the orthogonal transformation error between platform and geographical coordinates. The error state vector is written as follows:

$$\underline{x} = \left\{\varepsilon_N, \varepsilon_E, \varepsilon_D,\ \delta L,\ \delta \ell\right\} \tag{A-2}$$

where,

$\varepsilon_N$ = North component of attitude error

$\varepsilon_E$ = East component of attitude error

$\varepsilon_D$ = Vertical component of attitude error

$\delta L$ = Latitude error

$\delta \ell$ = Longitude error

The left hand side of the above error differential equation is written as:

$$\underline{\Lambda} = \left[\begin{array}{ccc|cc} & & & \dot{\lambda}\sin L & -\cos L\, p \\ & p\,\underline{I} + \underline{\Omega}^n_{in} & & p & 0 \\ & & & \dot{\lambda}\cos L & \sin L\, p \\ \hline 0 & f_D & -f_E & \delta f_N/\partial L & \delta f_N/\partial \ell \\ -f_D & 0 & f_N & \delta f_E/\partial L & \delta f_E/\partial \ell \end{array}\right] \tag{A-3}$$

where,

p = Differential operator, d/dt

$\underline{I}$ = Identity matrix

$f_N, f_E, f_D$ = North, East, and vertical components of the specific force vector, respectively.

$\underline{\Omega}^n_{in}$ = Skew-symmetric form of the angular velocity of the geographic framing relative to the inertial frame, resolved in geographic axes, and having the components:

$$\{\dot{\lambda}\cos L, \; -\dot{L}, \; -\dot{\lambda}\sin L\}$$

$\ell$ = Terrestrial longitude

$\dot{\lambda}$ = Celestial longitude rate $\left(\dot{\lambda}=\dot{\ell}+\omega_{ie}\right)$

L = Geographic latitude

The forcing function, $\underline{Q}$, which shows the effects of the inertial system's errors is given by:

$$\underline{Q} = \begin{bmatrix} \underline{C}^n_p \, (u)\underline{\omega}^p + \underline{C}^n_p \left\{\tau_x \dot{\lambda}\cos \dot{L}, \; -\tau_y \dot{L}, 0\right\} \\ \\ \underline{C}^n_p (u)\underline{f}^a \end{bmatrix} \qquad \text{(A-4)}$$

where,

$\underline{C}^n_p$ = coordinate transformation between platform and geographic axes

$$= \begin{bmatrix} \cos\phi & -\sin\phi & 0 \\ \sin\phi & \cos\phi & 0 \\ 0 & 0 & 1 \end{bmatrix}$$

$\phi = \int_0^t \dot{\lambda}\sin L \, dt$

$(u)\underline{\omega}^p$ = gyro drift uncertainty vector

$(u)\underline{f}^a$ = accelerometer uncertainty vector

$\tau_x, \tau_y$ = torquer scale factor uncertainty associated with the platform's x and y gyros, respectively.

It is seen from Eq. (A-3) that the equations of motion are time varying except for the case of constant east-west velocity at constant latitude where $\dot{\lambda}$ = constant and $\dot{L} = 0$. Note also that this system is insensitive to azimuth gyro torquing uncertainty, since, of course, the azimuth gyro is untorqued.

## APPENDIX B

## $N^*_{ay}$ EQUATION

The collision situation is characterized by the loss of separation in all three dimensions simultaneously. In concentrating on the risk due to lateral separation, we are considering aircraft travelling on nominally parallel tracks at the same level. Their along-track positions are presumed independent. The original formula for the number of accidents[9], derived from the work of P. G. Reich[6-8], is given by,

$$N_{ay} = 10^7 \left\{ E_y(\text{opp}) P_y(S_y) \frac{1}{S_x} \left[ \overline{V} P_z(0) + \lambda_x N_z(0) + \frac{\lambda_x |\overline{\dot{y}(S_y)}| P_z(0)}{2\lambda_y} \right] \right.$$

$$+ E_y(\text{same}) P_y(S_y) \frac{1}{S_x} \left[ \frac{1}{2} \overline{\Delta V} P_z(0) + \lambda_x N_z(0) \right.$$

$$\left. \left. + \frac{\lambda_x |\overline{\dot{y}(S_y)}| P_z(0)}{2\lambda_y} \right] \right\} \qquad \text{(B-1)}$$

where the parameters above are identified in Section 3.

The overlap probability, $P_y(S_y)$, and the relative velocity upon overlap, $\dot{y}(S_y)$, are directly related to the inertial navigation system flying errors, and hence to the direction of, and time into, flight. Proximate aircraft flying in the same direction are assumed to have equal elapsed navigation times and, therefore, identical flying statistics; on the other hand, for proximate aircraft travelling in opposite directions, there are distinct navigation times associated with each aircraft and, hence, different flying statistics. These features necessitate the adaptation of the model presented in equation (4), where the explicit dependence of $P_y$ and $\dot{y}$ on $S_y$ has been suppressed.

### PROBABILITY OF OVERLAP

The lateral overlap probability, $P_y(S_y)$, is obtained by convolving the flying densities of the laterally proximate aircraft[9]. Symbolically,

$$P_y(S_y) = 2\lambda_y \int_{-\infty}^{\infty} f_1\left(y - \frac{S_y}{2}\right) f_2\left(y + \frac{S_y}{2}\right) dy \qquad \text{(B-2)}$$

where $f_i(y)$ is the flying density of aircraft i about the center of its track and $\lambda_y$ is the lateral dimension of the aircraft.

The distribution of terminal errors, graphically represented in Figures 1 and 2, decays at a rate more slowly than Gaussian and more rapidly than exponential. The en route error distributions are assumed identical, in form, to the terminal distributions. Therefore, we have chosen a Gaussian random variable and a first-Laplacian (double-sided exponential) random variable as, respectively, optimistic and pessimistic models of the en route errors. The characteristics of both of these random variables are completely specified in terms of their second order statistics. They are assumed to have zero mean. Their variances - which are, of course, time dependent - were obtained by combining an error simulation model with the terminal data.

The Gaussian assumption, when combined with Equation (B-2) leads to:

$$P_y(S_y) = 2\lambda_y \int_{-\infty}^{\infty} \frac{1}{\sqrt{2\pi}\sigma_i(t_i)} e^{-\left(y - \frac{S_y}{2}\right)^2 / 2\sigma_1^2(t_1)}$$

$$\cdot \frac{1}{\sqrt{2\pi}\sigma_2(t_2)} e^{-\left(y + \frac{S_y}{2}\right)^2 / 2\sigma_2^2(t_2)} dy \qquad \text{(B-3)}$$

where $\sigma_i(t_i)$ is the standard deviation of the en route Gaussian navigation errors in aircraft i at time $t_i$. The final result is very much a function of the times $t_1$ and $t_2$, though this dependence has been suppressed for notational convenience. Equation (B-3) can be shown to reduce to:

$$P_y(S_y) = \frac{\lambda_y e^{-\frac{1}{2}\frac{S_y^2}{\left[\sigma_1^2(t_1) + \sigma_2^2(t_2)\right]}}}{\sqrt{\frac{\pi}{2}\left[\sigma_1^2(t_1) + \sigma_2^2(t_2)\right]}} \qquad \text{(B-4)}$$

For an opposite-direction lateral proximity, the two flight times were related to one another. The $\sigma$ values for both the easterly and westerly flights were obtained from Figure 3 - or a scaled version thereof. For the case of same-direction proximity, we assumed $t_1 = t_2$ and since the direction is also the same, $\sigma_1(t_1) = \sigma_2(t_2)$. Here, the overlap probability is seen to reduce to:

$$P_y(S_y) = \frac{\lambda_y e^{-\frac{1}{4}\frac{S_y^2}{\sigma^2(t)}}}{\sqrt{\pi}\,\sigma(t)} \qquad \text{(B-5)}$$

The exponential case was treated in an analogous manner. Solving,

$$P_y = 2\lambda_y \int_{-\infty}^{\infty} \frac{1}{\sqrt{2}\sigma_1(t_1)} e^{-\frac{|y - \frac{1}{2}S_y|}{\sigma_1(t_1)}} \cdot \frac{1}{\sqrt{2}\sigma_2(t_2)} e^{-\frac{|y + \frac{1}{2}S_y|}{\sigma_2(t_2)}} dy \qquad \text{(B-6)}$$

we obtained:

$$P_y(S_y) = \frac{\lambda_y}{\sqrt{2}} \left\{ \frac{1}{\sigma_1(t_1) + \sigma_2(t_2)} \left[ e^{-\sqrt{2}\,\frac{S_y}{\sigma_1(t_1)}} + e^{-\sqrt{2}\,\frac{S_y}{\sigma_2(t_2)}} \right] \right.$$

$$\left. + \frac{1}{\sigma_1(t_1) - \sigma_2(t_2)} \left[ e^{-\sqrt{2}\,\frac{S_y}{\sigma_2(t_2)}} - e^{-\sqrt{2}\,\frac{S_y}{\sigma_1(t_1)}} \right] \right\} \qquad \text{(B-7)}$$

For the same direction case, this can be shown to reduce to:

$$P_y(S_y) = \frac{\lambda_y}{\sigma(t)}\, e^{-\sqrt{2}\,\frac{S_y}{\sigma(t)}} \left[ \frac{1}{\sqrt{2}} + \frac{S_y}{\sigma(t)} \right] \qquad \text{(B-8)}$$

a result derived by Reich in reference (7).

PARAMETER VALUES

The values used in this analysis are presented in Table B-1 below, along with a brief explanation of their source.

| Parameter | Assigned Value | Explanation/Source |
|---|---|---|
| $E_y^e$ (same) | 0.417 | Reference 12; uses average daily traffic forecasts (for 1975) obtained from Reference 11 and a longitudinal proximity of 120 n.m. |
| $E_y^w$ (same) | 0.417 | |
| $E_y$ (opp) | 0.014 | |
| $S_x$ | 120 n.m. | Assumed longitudinal proximity distance |

| Parameter | Assigned Value | Explanation/Source |
|---|---|---|
| $N_z(0)$ | 20 cycl/hr | Reference 10 |
| $P_z(0)$ | .25 | Reference 10 |
| $\overline{V}$ | 560 knots | ~ Average of carriers; increase over value used in reference 10; slightly inconsistent with the 637 knots, used for mathematical convenience in the INS analysis (results are essentially unnaffected). |
| $\overline{\Delta V}$ | 15 knots | Slightly more conservative than value given, reference 10. |
| $\lambda_y$ | .033 n.m. | ~ Average of carriers; larger than reference 10 value. |
| $\lambda_y$ | .033 n.m. | ~ Average of carriers (ignoring vortex); larger than reference 10 value. |
| $\lvert\dot{y}^e(\text{same})\rvert$<br>$\lvert\dot{y}^w(\text{same})\rvert$<br>$\lvert\dot{y}(\text{opp})\rvert$ | functions of time (See Figure 4 and Table 2) | Velocity errors are scaled by the ratio of the aircraft's actual position error upon overlap to its expected error. |

COMPUTER PROGRAMS

The en route INS errors were simulated on the IBM 7094. The solution of $N^*_{ay}$ (Equation (4)) was programmed on the Tymeshare time sharing facilities.

## REFERENCES


1. "Rapport D'Experimentation Des Centrales a Inertie Litton LTN-51 Sur B.707"; Air France Report DO.NT, 1970.

2. Laning, J. H. and Battin, R. H.; Random Processes in Automatic Control; McGraw-Hill, 1956.

3. Pitman, G. R., Inertial Guidance; John Wiley and Sons; 1962.

4. Britting, K. R.; Inertial Navigation Systems Analysis; John Wiley & Sons, 1971 (In Press).

5. Dushman, A.; "On Gyro Drift Models and Their Evaluation", I.R.E. Trans On Aerospace and Navigational Electronics; December, 1962.

6. "Analysis of Long-Range Air Traffic Systems: Separation Standards - I", P. G. Reich, Journal of the Institute of Navigation, Vol. 19, No. 1, January 1966.

7. "Analysis of Long-Range Air Traffic Systems: Separation Standards - II", P. G. Reich, Journal of the Institute of Navigation, Vol. 19, No. 2, April, 1966.

8. "Analysis of Long-Range Air Traffic Systems: Separation Standards - III", P. G. Reich, Journal of the Institute of Navigation, Vol. 19, No. 3, July, 1966.

9. "Summary of Discussions of the Second Meeting of the NAT Systems Planning Group", December, 1966.

10. "Summary of Discussions of the Fourth Meeting of the NAT Systems Planning Group", June, 1968.

11. "The Role of User Operational Penalties in the Assessment of Future Ocean System Modifications", Chester Dunmire, Draft Report, June 1969.

12. "Studies of Traffic Packing for Estimating Mid-Air Collision Risk over the North Atlantic", P. P. Scott, Royal Aircraft Establishment Technical Report 68097, April, 1968.